JMEPEG
DOI: 10.1007/s11665-012-0451-5

1059-9495/$19.00

Finite Element Analysis of Material Flow in Mechanical Clinching with Extensible Dies

Francesco Lambiase and Antoniomaria Di Ilio

(Submitted June 28, 2012; in revised form October 23, 2012)

An investigation of the material flow during the clinching process with extensible dies is carried out. Clinched joints were produced under different forming loads to evaluate the evolution of the joints' profile experimentally. Tensile-shear tests were conducted to evaluate the influence of the forming load on mechanical strength of the clinched joint. Since the joints' strength depends on the joints' profile, which in turn depends on the punch-die cavity volume, an analysis of the forces acting on the extensible dies was carried out. A finite element model was developed and validated by comparing the predicted and measured material flow and quality criteria (e.g., neck thickness and undercut). Therefore, the FE model was utilized to analyze the evolution of contact forces acting on the die sectors during the joining process. Furthermore, the main causes of the asymmetry in the cross section of such joints have been studied. It turned out that the axial asymmetry due to material flow within the gap between consecutive die sectors increases with the punch force and the sheet thickness.

Keywords clinching, extensible die, joining, mechanical fastening

1. Introduction

In the recent years, the research in the field of mechanical joining of metal sheets has gained considerable attention due to the employment of materials which are difficult to join by welding (for example, joining different materials having different melting points). In the automotive industry, self-pierce riveting and mechanical clinching are being successfully employed. Self-pierce riveting consists of forcing a rivet directly within two sheets without the employment of a predrilled hole, thus allowing a remarkable cut-off of run time (which is almost 1 s). Mechanical clinching is intended to produce a geometrical interlock between the sheets by producing an appropriate material flow with a punch and the die. Recently, Mori et al. (Ref 1) performed a comparison between the static and fatigue strength of joints produced with clinching and self-pierce riveting; clinched joints exhibited a lower static strength as compared to self-pierced rivets, but a similar fatigue strength. In particular, the examined clinched joints showed a cross-tensile strength 2.7 times lower than those produced with self-pierce riveting; however, the latter required a forming load three times higher than that required by the clinching process. Thus, the employment of mechanical clinching would allow the usage of low power machines (even portable equipment) or equal available maximum load to produce a higher number of clinched joints with a single stroke. Furthermore, mechanical clinching does not require the employment of subsidial material such as rivets, thus permitting a significant reduction of costs (Ref 2) and run time (Ref 1). Clinched joints' failure mechanisms were identified by Varis (Ref 3) and an analytical model to predict the clinched joints' strength was proposed in Ref 4. It was found that clinched joints may undergo mainly two types of failures, namely unbutton and neck fracture. The occurrence of the first or second failure mode depends on the produced undercut and thickness of the upper sheet of the clinched joint profile. Therefore, several investigations have been carried out to evaluate the effect of process parameters on the final clinching profile (Ref 5), and an automatic optimization of process parameters approach was presented in Ref 6. Because of the its advantages, several investigations have been carried out in the last decade to widen the availability of the clinching process to new materials, leading to the proposal of new tools configurations. Abe et al. (Ref 7) and Neugebauer et al. (Ref 8) have adopted flat dies to join high strength steels, aluminum, and magnesium alloys to avoid fracture. Mechanical clinching has been successfully implemented on polymer components (Ref 9). A comparison among some configurations including grooved dies and extendible dies with round and square punch clinching was carried out in Ref 10; however, the forming conditions were not clarified.

In the present study, the material flow produced in the clinching process using an extensible die is analyzed. To this end, clinched joints were carried out under different forming loads. The joints were cross-sectioned and the main geometrical dimensions, e.g., the undercut and the neck thickness, influencing the mechanical characteristics of the joints were determined. Shear-tensile tests were also performed to evaluate the effect of forming load on mechanical behaviors of the clinched joints. A FE model was developed to analyze the material flow and the change of cross section due to the unsymmetrical material flow. Since the clinched joint profile depends on the punch-die cavity volume (shape and

Francesco Lambiase and **Antoniomaria Di Ilio**, Department of Mechanical Energy and Management Engineering, University of L'Aquila, 67040 Monteluco di Roio, AQ, Italy. Contact e-mail: francesco.lambiase@univaq.it.

Published online: 12 December 2012

dimensions), the FE model was also utilized to gather a better insight into the variation of contact force on the die sectors, which influences the die sectors' displacement.

2. Mechanical Clinching Background

The clinching process is intended to realize a mechanical interlock between two or more sheets by producing an appropriate localized deformation of the sheets with the aid of a punch and a die. Different configurations have been presented so far, mainly differentiating in the die scheme, e.g., round grooved die, square die, flat die, and extensible die. During the joint formation, the upper sheet (which is in contact with the punch) undergoes a significant thinning near the punch corner radius. Thus, the static and fatigue strengths of clinched joints depend on the clinched joint profile (Ref 1, 11-16) and particularly on the final thickness of the upper sheet near the punch corner, namely neck thickness (t_n), and the magnitude of the produced undercut (t_s) depicted in Fig. 1. The proper design of mechanical clinching tools is aimed at maximizing such quality criteria at the end of the process (Ref 4, 17). In addition, from a process viewpoint, the forming force from which the energy consumption is derived is achieving more and more consideration in process development and optimization. One of the first investigations carried out considering the required forming force was developed by Mucha (Ref 15), which analyzed the main clinching tools' geometrical parameters affecting the forming force. To this end, the influence of forming force on clinched joints' geometrical and mechanical characteristics was investigated.

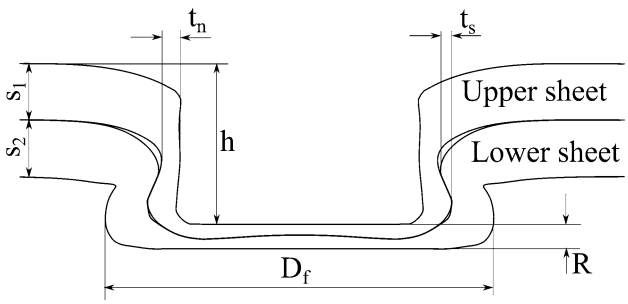

Fig. 1 Main geometrical characteristics of clinched joints profiles

The mechanical strength of clinched joints depends on the produced joint profile other than the mechanical behavior of material and process-induced strain hardening. The clinching

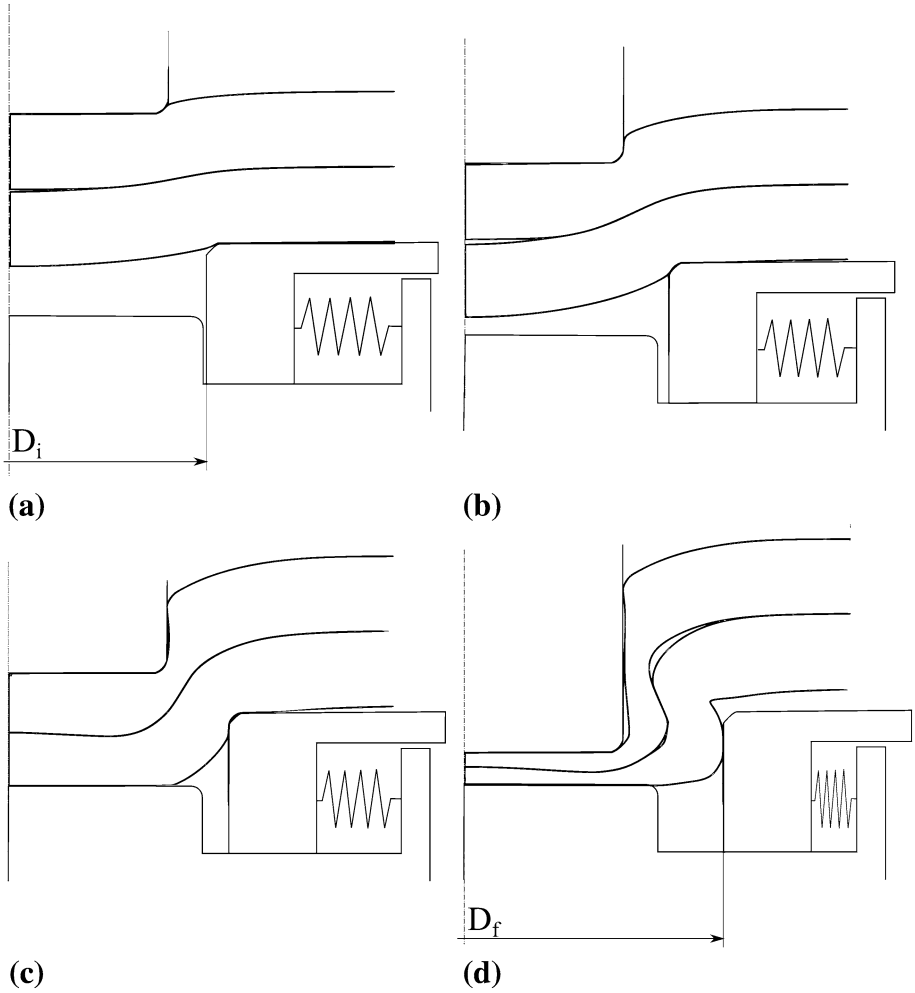

Fig. 2 Clinching phases with extensible dies: (a) early bending; (b) drawing; (c) radial spreading with radial movement of the die becoming evident; (d) early occurrence of indirect extrusion

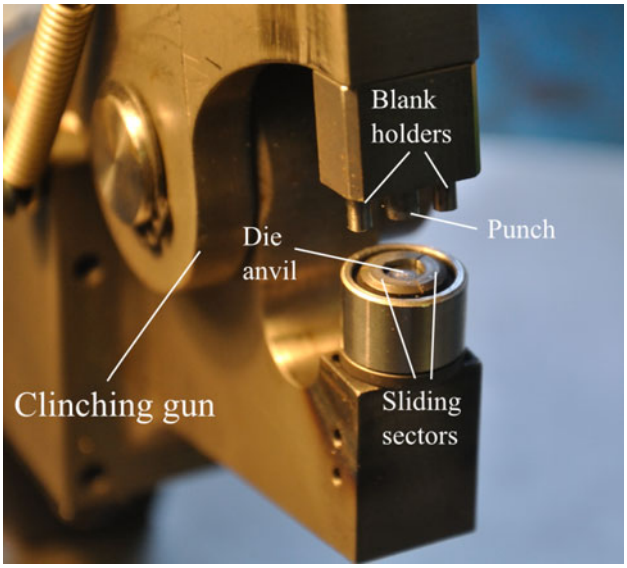

Fig. 3 Experimental clinching equipment

process with extensible dies evolves through four phases as depicted in Fig. 2: (a) localized plastic deformation of the upper and lower sheets, (b) drawing, (c) radial spreading, and (d) indirect extrusion. Initially, the upper sheet near the punch corner deforms plastically, undergoing a significant thinning under a slight punch stroke; similarly, the lower sheet which is forced against the die corner radius undergoes a localized plastic deformation. A larger punch stroke produces a major radial sliding of die sector and the cavity volume enlarges. As the lower sheet comes up against the die anvil, Fig. 2(c), a large radial material flow of both sheets takes place and the die sectors slide more relevantly. During the last phase, the undercut between the upper and lower sheet is formed as depicted in Fig. 2(d) and a little reduction of neck thickness still occurs.

3. Materials and Methods

Mild steel sheets with a nominal thickness of 1.0 mm were joined by mechanical clinching using extensible and fixed dies, and then static characterization tests were performed. The extensible die (provided by Jurado Corporation, Perugia, Italy) is constituted by a fixed die anvil having a diameter $D = 5.4$ mm and three sliding sectors having a minimum diameter $D_i = 5.75$ mm and a corner radius $R = 0.2$ mm. A punch having a diameter $d = 4.1$ mm and a corner radius $r = 0.2$ mm was employed in the experiments. The experimental equipment is depicted in Fig. 3. The mechanical properties of the steel sheets were measured by performing tensile tests according to ASTM Standards (ASTM E8) for sheet type specimens with different angles between the loading direction and the rolling one. The engineering stress-strain curves achieved by the tensile tests are depicted in Fig. 4.

Shear tensile tests were performed on joints produced under different forming conditions in order to evaluate their mechanical properties. The tests were developed on a servo-hydraulic universal machine using a load cell having a 25 kN full scale, with a cross-head speed of 0.2 mm/s. The joint failure was defined as the complete separation of the sheets. A schematic of

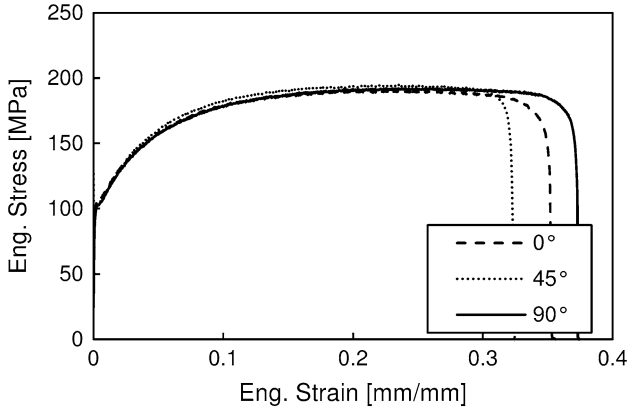

Fig. 4 Stress-strain relationship of the analyzed material under different loading directions to rolling one

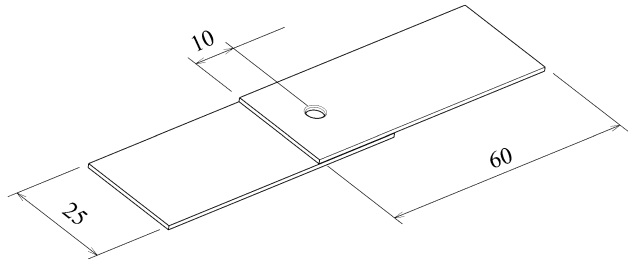

Fig. 5 Schematic of samples used for tension-shearing characterization tests (the reported dimensions are expressed in millimetres)

the specimen used for the tension-shearing tests is illustrated in Fig. 5.

4. Modeling Approach

An elasto-plastic behavior was assumed for the sheets' material, while the clinching tools behave rigidly. The little planar anisotropy showed by the material was not taken into account in the simulation. The constitutive equation representing the sheet material strain hardening is presented in the conventional Ludwik's equation reads $\sigma_p = \sigma_0 + K\varepsilon_p^n$ is used to describe the work hardening; σ_p and ε_p are the equivalent stress and equivalent strain, respectively. The material parameters σ_0 (initial yield stress 67 MPa), K (strength coefficient 309 MPa), and n (work-hardening coefficient 0.314) are determined by fitting the stress-strain curve obtained from uniaxial tensile test along the rolling direction. The constant K is structure dependent and is influenced by processing, while n is a material property normally lying between 0.1 and 0.6 (Ref 18). Because the clinch joint dimensions are of the same order of magnitude as sheets' thickness, the simulation must be conducted as a bulk metal forming process. A 3D model with one plane of symmetry was developed to analyze the material flow during the joining process. Different mesh densities have been tested and a mesh pattern having almost 50000 elements with refined zones (the average element size of the upper sheet near the punch corner radius was 0.03 mm) was found to be accurate enough to predict the clinch profile. Frequent adaptive

remeshing steps were needed to preserve the mesh from the excessive element distortion that usually occurs in clinching simulations (Ref 19). A kinematic contact algorithm was adopted to simulate the interaction between sheets and tool-sheet contacts because of the extremely large values of compressive stress that are generally encountered, which is the main reason of avoiding a penalty contact formulation employment. In FE modeling of the clinching process, the friction coefficients are assumed uniform between the contact surfaces shared by clinching tools and the sheets, which is not properly true in the real process. Hence, the friction coefficient to be used can be retained as an average value comprising a combination of phenomenological and numerical issues. A Coulomb friction model with $\mu = 0.15$ was assumed at the sheet-tool interfaces except that of the lower sheet-die anvil which was $\mu = 0.25$. Indeed, a series of furrows were realized on the die anvil to reduce the radial flow of lower sheet material. As a matter of fact, such an expedient permits the achievement of a larger contact surface between the upper and lower sheets (avoiding the formation of voids) near the undercut area. Several values of mass scaling factor were tested and a value of 100 was preferred since it allowed a

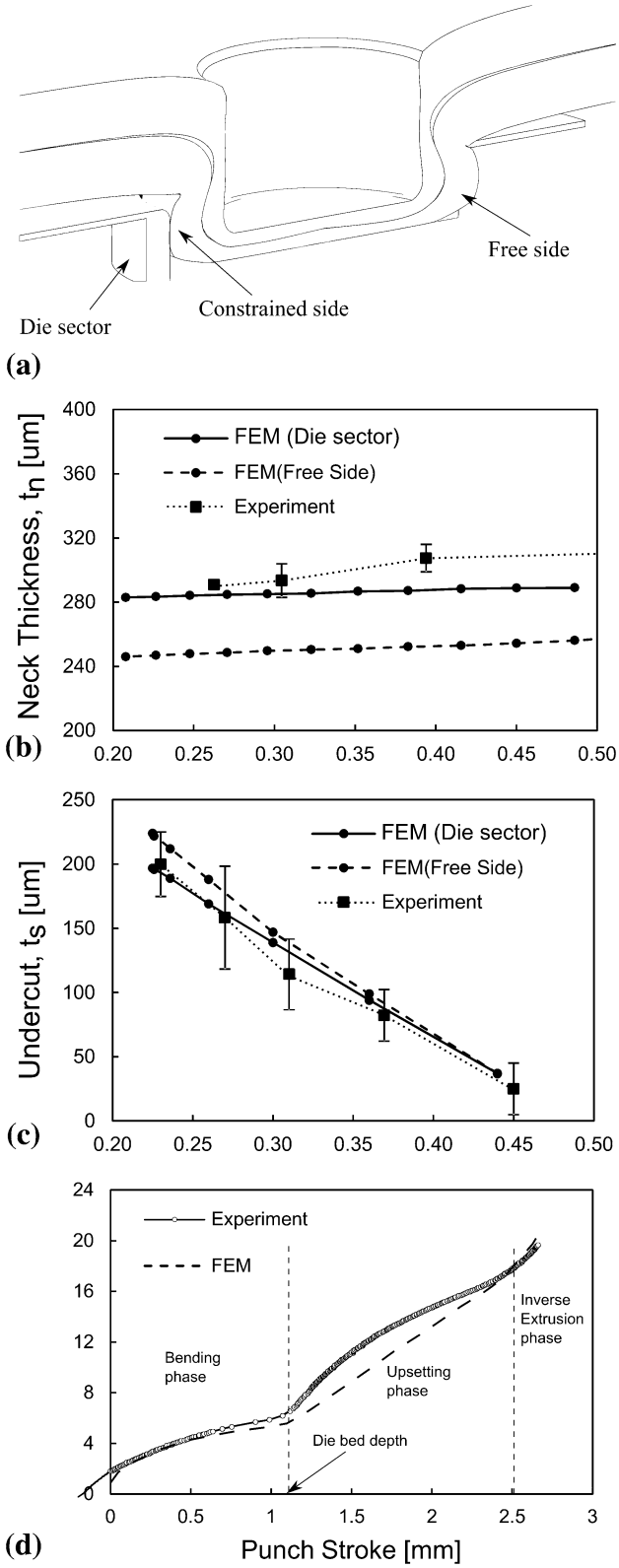

Fig. 6 (a) schematic representation of the cross section of a clinched joint. Evolution of (b) neck thickness and (c) undercut with bottom thickness of the joint, (d) evolution of forming load with punch stroke. The normalized bottom thickness $X = R/(s1 + s2)$

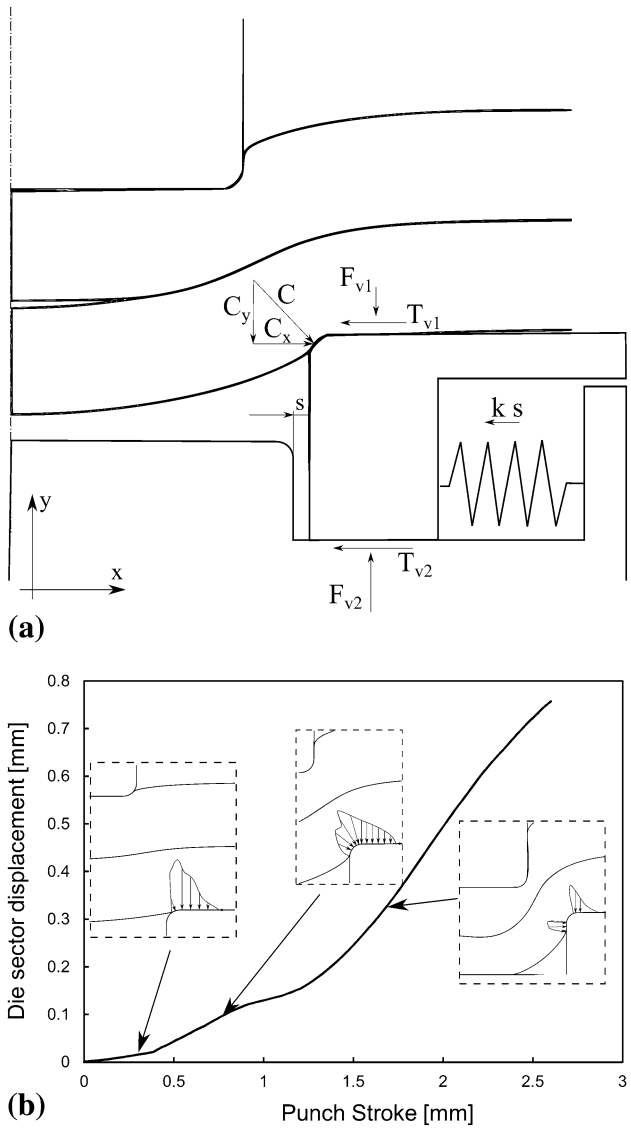

Fig. 7 (a) System of forces acting on the movable die sector; (b) evolution of contact forces of die sector

remarkable cut-off of the simulation time without introducing significant inertial effects in simulations.

5. Results and Discussion

5.1 Model Validation

Before showing the simulation results, a brief discussion of model accuracy is reported. The validation of the numerical model involves the comparison of experimental measurements with the predictions of the developed model concerning the geometrical characteristics, i.e., undercut, neck thickness, and bottom thickness of the joint other than the evolution of the forming load. The measurements of the neck thickness and undercut were performed by sectioning the clinched joints (three repetitions for each processing condition) along a random axial plane. On the other hand, the numerical values of such quality criteria were extracted from the middle of the die sector and the middle of die sectors gap as reported in Fig. 6(a).

A reasonable agreement between the FE model results and experimental data was observed for all the analyzed parameters, as shown in Fig. 6(b)-(d); however, a little difference between the FE model prediction and experimental measurement can be observed regarding the evolution of the forming load with the punch stroke. Indeed, after the bending/drawing phase, the experimental curve exhibits a knee which was not shown by the FE model results; such a discrepancy was addressed to the neglecting of the material transverse anisotropy.

The clinched joint profile and particularly the neck thickness are directly influenced by the evolution of material flow during the initial forming phase. Indeed, the larger the cavity volume,

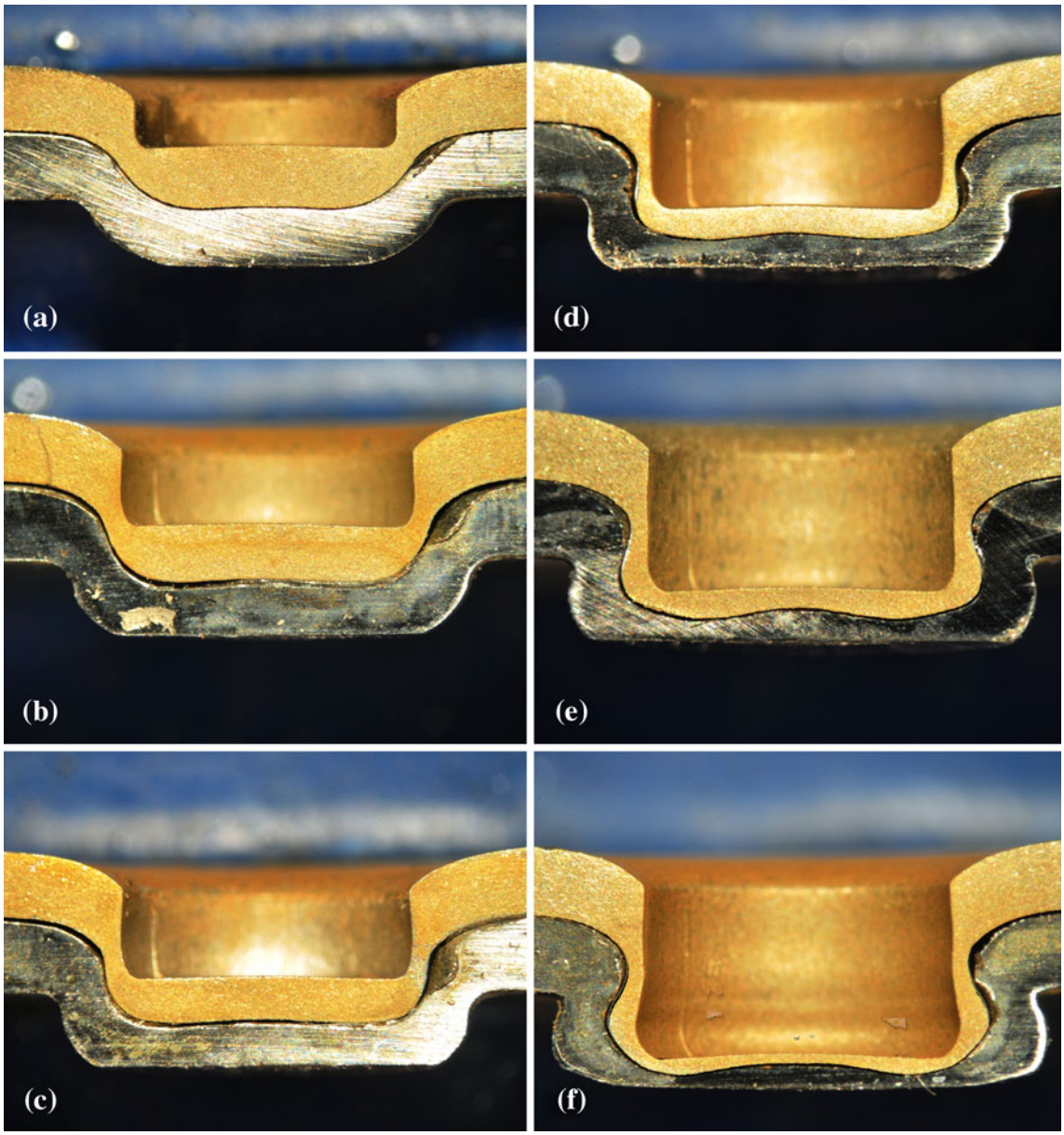

Fig. 8 Material flow produced with the extensible die under different forming loads: (a) $F = 8$ kN, (b) $F = 12$ kN, (c) $F = 14$ kN, (d) $F = 18$ kN, (e) $F = 22$ kN, and (f) $F = 24$ kN. In order to better distinguish the upper from the lower sheet, the upper sheet was painted with gold color

the lower the thinning effect on the upper sheet, and in turn the larger the neck thickness at the end of the process. However, an excessive large cavity volume would reduce the magnitude of the developing undercut. When the extensible dies are adopted, the cavity volume modifies during the process. Indeed, the radial displacement of the die sectors s (and in turn, the punch-die cavity volume) depends on the developing system of forces acting on the moving dies' surfaces. The die sector is subjected to the contact pressure acting on the flat surface F_{v1} and on the die knee C, the tangential friction force on the flat surface $T_{v1} = F_{v1} \cdot \mu$, the vertical contact force $F_{v2} \sim F_{v1} + C_y$, the friction force $T_{v2} = F_{v2} \cdot \mu$, and the elastic reaction of the spring $k \cdot s$, other than a negligible tangential force on the die knee. A schematic representation of the forces acting on a movable die sector is reported in Fig. 7(a). During the first phases of the process, the horizontal component of contact pressure is almost null; thus, a negligible displacement of the die sector is produced. As the punch stroke increases, the horizontal component of contact pressure becomes more relevant, determining a larger displacement of the die sector as depicted in Fig. 7(b), and in turn the punch-die cavity volume enlarges. As the lower sheet comes in contact with the die anvil, the vertical component of contact pressure acting on the movable sector (C_y) is further reduced and the cavity volume enlarges. Such behavior is also evident on the cross sections (along random axial planes) performed on the experimental samples produced under different forming loads, as depicted in Fig. 8. In addition, as the forming force increases, the axial asymmetry of the joint profile increases due to the developing material flow rather than some technological issues, e.g., punch-die loss of coaxially. Indeed, as the forming load increases, the radial spreading of the extensible die becomes relevant and part of the material flows between the die sectors' gap.

The increase of axial asymmetry with the forming load is more evident from the bottom view of the clinched joint as reported in Fig. 9. As can be observed, under high forming loads, the extensible die imparts an unsymmetrical shape to the clinched joint because of the material flows along the die sectors gaps. Indeed, as the punch-die cavity volume is fulfilled, the die sectors slide away from the die anvil, leaving part of the material to flow within such gaps. Then, the final shape of the clinched joint becomes highly axially unsymmetrical.

The change of cross-sectional profile particularly the undercut and neck thickness along the clinched joint length was investigated numerically. Since the examined extensible die is composed by three sectors disposed at 120°, the change of neck thickness and undercut is analyzed from the middle of a die sector (constrained side) to the middle of the sectors' gap (free side). Starting from the most constrained side ($\alpha = 0$), as shown in Fig. 10, the undercut shows its minimum, then it increases up to its maximum value as moving toward the free side. However, a little drop of the undercut occurs within the free side ($\alpha = 60°$). The neck thickness seems to follow just the opposite trend as compared to that of the undercut. Indeed, as the die shoulders (on the die sectors) restrain the radial motion of the lower sheet and in turn the radial motion of the upper one, a larger undercut is produced in weaker constrained zones. Likely, since a larger material flow in the radial direction of both the upper and lower sheets is produced within the die sectors gap, a thinner neck is produced in correspondence to such "constrain-free" zones.

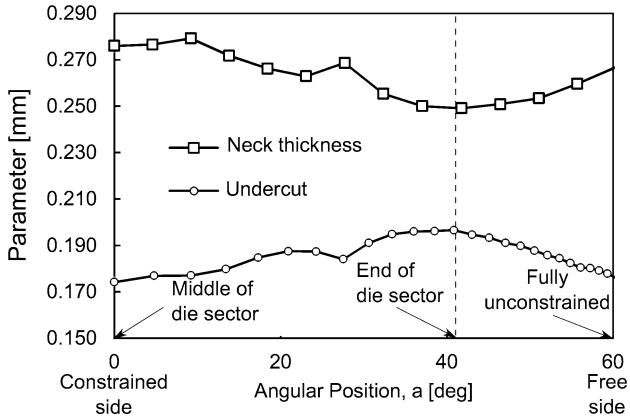

Fig. 10 Change of neck thickness and undercut along hoop direction

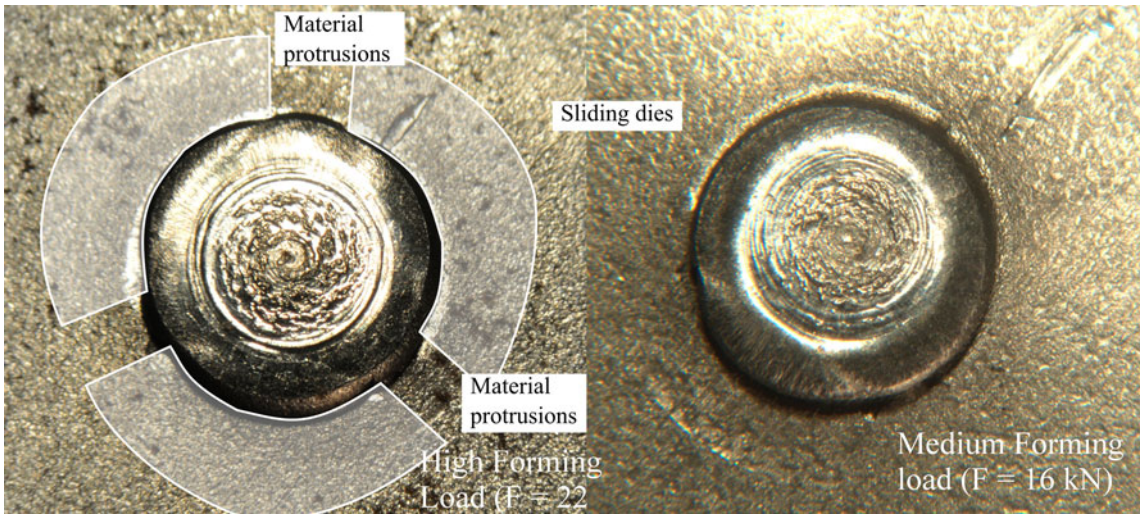

Fig. 9 Bottom view of clinched samples with extensible and grooved dies

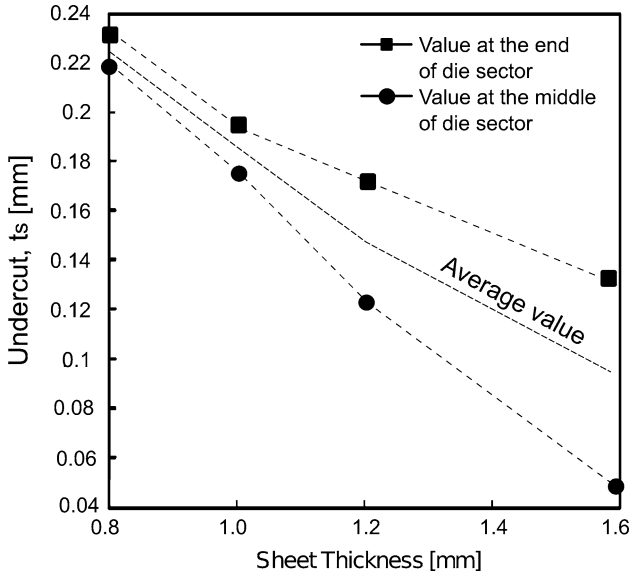

Fig. 11 Influence of sheet thickness on undercut as calculated by numerical model

The analysis of metal flow was also performed on sheets having different thicknesses, i.e., 0.8 + 0.8, 1.2 + 1.2, and 1.6 + 1.6 mm (other than 1.0 + 1.0 mm). As can be noted in Fig. 11, the thicker the sheets, the lower the produced undercut, and the larger its variability along the join length. The variation of the undercut with sheet thickness is mainly due to an insufficient punch-die cavity volume which leads to extremely low values of undercut especially for higher values of sheet thickness, e.g., t = 1.2 +1.2 and even more evident when t = 1.6 + 1.6.

Thicker sheets involve a larger material flow within the cavity volume, which in turn encompass a larger radial displacement of the die sectors as depicted in Fig. 12. Therefore, a larger gap between the sectors is produced, allowing a larger material flow outside the cavity volume. The increase of the change of the undercut with the sheet thickness can be addressed to such a higher material flow between the extensible die sectors which determine a higher divergence between the radial displacement (and thus the undercut) of the most and less constrained areas of the joint.

The variation of separation force during the experimental shear tests is reported in Fig. 13. As can be noted, the first part of the curves (which characterizes the stiffness of the joint) is

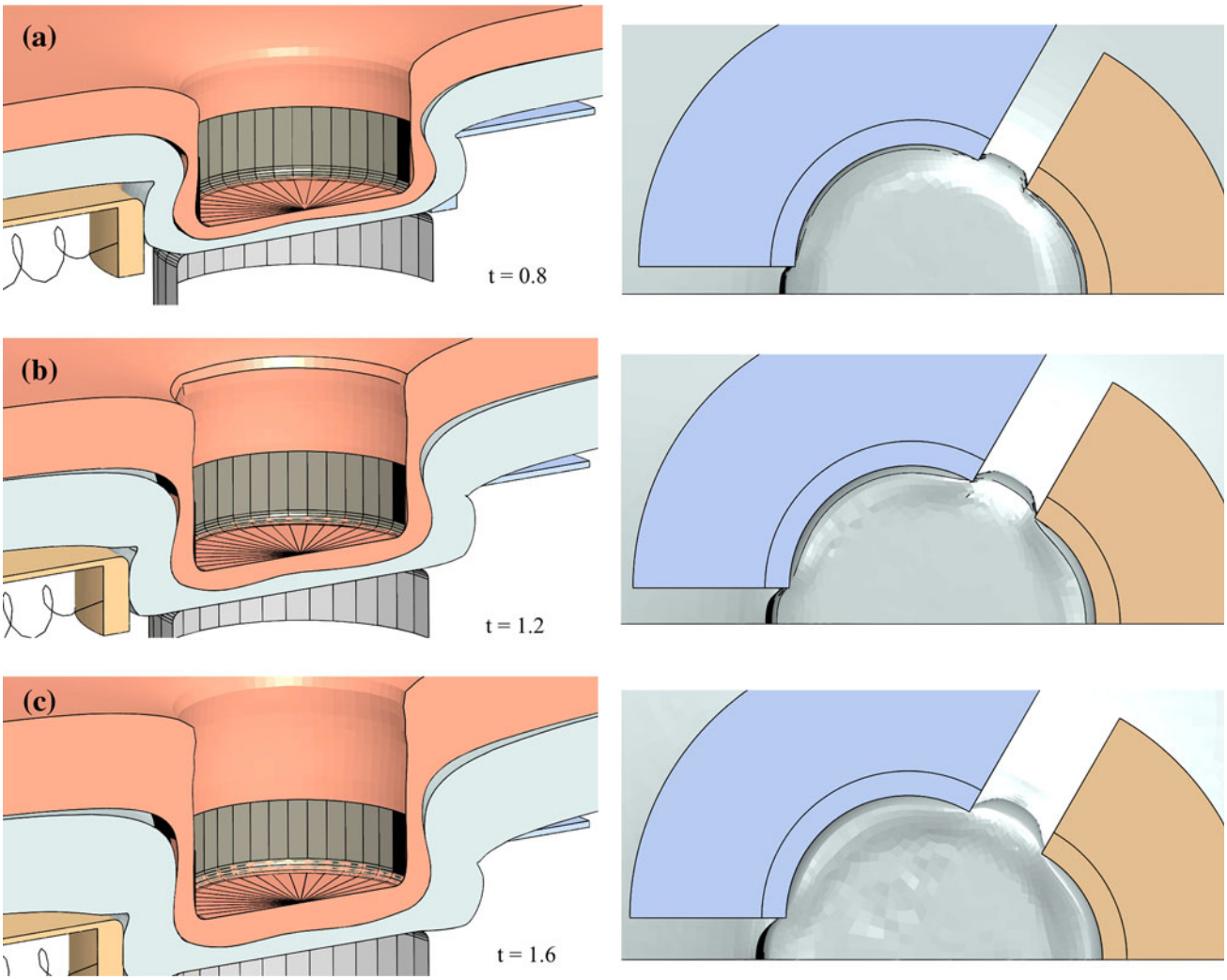

Fig. 12 Material flow produced with different values of sheet thicknesses

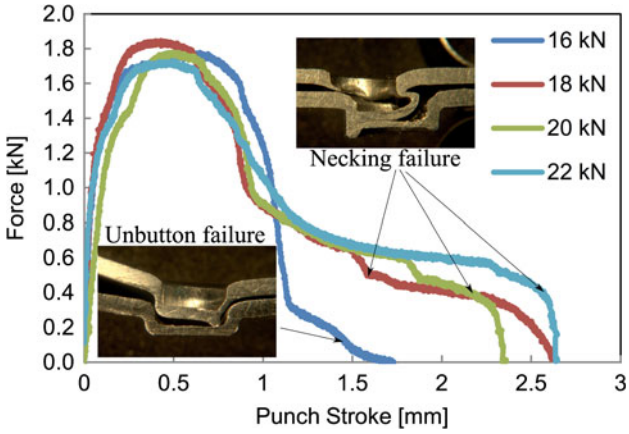

Fig. 13 Evolution of separation force during shear tensile tests of joints produced under different forming loads

almost identical regardless of the involved processing conditions. Conversely, a limited difference appears up to achieving the maximum joint strength. After the force peak, the curves' drops are very close except for that of the joint produced under the lowest forming load, i.e., $F = 16$ kN, which undergoes a steeper drop. Indeed, such a joint separated due to unbutton, while all the others failed due to upper sheet necking which is more gradual (because of the relatively high ductility of the involved steel material). Concerning the joint strength, it undergoes a little increase when the forming load is increased up to 18 kN and then it decreases. Indeed, the undercut produced with a forming load of 16 kN is relatively small. As a consequence, a little increase of the forming load (up to 18 kN) leads to an increase of undercut and in turn an increase of the joint strength. On the other hand, the increase of the forming load comes with a reduction of the neck thickness; therefore, a further increase of forming load leads to a lower resistant area of upper sheet, which in turn determines a reduction of the joint strength.

6. Conclusions

The clinching process with extensible dies has been analyzed. The material flow was investigated both experimentally and numerically. It was discovered that the main quality criteria on which the joint strength depends vary in the hoop direction due to different boundary conditions produced by the die sectors' displacement. Indeed, the undercut increases in the proximity of the die sector edge, while on the contrary the neck thickness assumes its minimum value just in that area, such behaviors being addressed to a weaker constraining effect in the radial direction.

During the early stages of the joining process, the material flow produced with the extensible dies is relatively similar to that produced with fixed dies because of the negligible radial displacement of the die sectors. However, as the process proceeds, a substantial increase of punch-die cavity volume takes place (because of the considerable radial displacement of the die sector) giving rise to an enlargement of the top head of the clinched joint.

The analysis of material flow has allowed to establish that higher forming forces and thicker sheet induce a larger axial asymmetry of the clinched joints since a larger material flow is produced.

References

1. K. Mori, Y. Abe, and T. Kato, Mechanism of Superiority of Fatigue Strength for Aluminium Alloy Sheets Joined by Mechanical Clinching and Self-Pierce Riveting, *J. Mater. Process. Technol.*, 2012, **212**(9), p 1811–1988
2. J. Varis, Economics of Clinched Joint Compared to Riveted Joint and Example of Applying Calculations to a Volume Product, *J. Mater. Process. Technol.*, 2006, **172**(1), p 130–138
3. J. Varis, Ensuring the Integrity in Clinching Process, *J. Mater. Process. Technol.*, 2006, **174**(1–3), p 277–285
4. C.-J. Lee, J.-Y. Kim, S.-K. Lee, D.-C. Ko, and B.-M. Kim, Design of Mechanical Clinching Tools for Joining of Aluminium Alloy Sheets, *Mater. Des.*, 2010, **31**(4), p 1854–1861
5. C.-J. Lee, J.-Y. Kim, S.-K. Lee, D.-C. Ko, and B.-M. Kim, Parametric Study on Mechanical Clinching Process for Joining Aluminum Alloy and High-Strength Steel Sheets, *J. Mech. Sci. Technol.*, 2010, **24**, p 123–126
6. M. Oudjene, L. Benayed, A. Delameziere, and J. Batoz, Shape Optimization of Clinching Tools Using the Response Surface Methodology with Moving Least-Square Approximation, *J. Mater. Process. Technol.*, 2009, **209**(1), p 289–296
7. Y. Abe, K. Mori, and T. Kato, Joining of High Strength Steel and Aluminium Alloy Sheets by Mechanical Clinching with Dies for Control of Metal Flow, *J. Mater. Process. Technol.*, 2012, **212**(4), p 884–889
8. R. Neugebauer, C. Kraus, and S. Dietrich, Advances in Mechanical Joining of Magnesium, *CIRP Ann. Manuf. Technol.*, 2008, **57**(1), p 283–286
9. M. Grujicic, V. Sellappan, G. Arakere, N. Seyr, A. Obieglo, M. Erdmann, and J. Holzleitner, The Potential of a Clinch-Lock Polymer Metal Hybrid Technology for Use in Load-Bearing Automotive Components, *J. Mater. Eng. Perform.*, 2008, **18**(7), p 893–902
10. J.P. Varis, The Suitability of Clinching as a Joining Method for High-Strength Structural Steel, *J. Mater. Process. Technol.*, 2003, **132**, p 242–249
11. H.-K. Kim, Fatigue Strength Evaluation of the Clinched Lap Joints of a Cold Rolled Mild Steel Sheet, *J. Mater. Eng. Perform.*, 2012. doi:10.1007/s11665-012-0232-1
12. S. Coppieters, P.Lava, R.V. Hecke, S. Cooreman, H. Sol, P.V. Houtte, and D. Debruyne, Numerical and Experimental Study of the Multi-Axial Quasi-Static Strength of Clinched Connections. *Int. J. Mater. Form.*, 2012. doi:10.1007/s12289-012-1097-4
13. S. Coppieters, P. Lava, S. Baes, H. Sol, P. Van Houtte, and D. Debruyne, Analytical Method to Predict the Pull-Out Strength of Clinched Connections, *Thin-Walled Struct.*, 2012, **52**, p 42–52
14. T.K. Pal and K. Bhowmick, Resistance Spot Welding Characteristics and High Cycle Fatigue Behavior of DP 780 Steel Sheet, *J. Mater. Eng. Perform.*, 2011, **21**(2), p 280–285
15. J. Mucha, The Analysis of Lock Forming Mechanism in the Clinching Joint, *Mater. Des.*, 2011, **32**(10), p 4943–4954
16. S. Coppieters, S. Cooreman, P. Lava, H. Sol, P.V. Houtte, and D. Debruyne, Reproducing the Experimental Pull-Out and Shear Strength of Clinched Sheet Metal Connections Using FEA, *Int. J. Mater. Form.*, 2010, **4**(4), p 429–440
17. F. Lambiase, Influence of Process Parameters in Mechanical Clinching with Extensible Dies, *Int. J. Adv. Manuf. Technol.*, 2012. doi:10.1007/s00170-012-4486-4
18. W.F. Hosford and R.M. Caddell, *Metal Forming: Mechanics and Metallurgy*, 3rd ed., Cambridge University Press, New York, 2007
19. V. Hamel, J.M. Roelandt, J.N. Gacel, and F. Schmit, Finite Element Modeling of Clinch Forming with Automatic Remeshing, *Comput. Struct.*, 2000, **77**, p 185–200